Available online at www.sciencedirect.com
SCIENCE DIRECT®

Journal of the European Ceramic Society 24 (2004) 2061–2066

www.elsevier.com/locate/jeurceramsoc

Centrifugal sintering of ceramics

Y. Kinemuchi[a,*], K. Watari[a], K. Uchimura[b]

[a] *Advanced Sintering Technology Group, Ceramics Research Institute, National Institute of Advanced Industrial Science and Technology, Moriyama, Nagoya 463-8560, Japan*

[b] *Shinto V-Cerax, Ltd., Honohara, Toyokawa 442-8506, Japan*

Received 11 January 2003; received in revised form 6 April 2003; accepted 13 April 2003

Abstract

We have proposed a new centrifugal sintering technology, which consists of heating and simultaneous high-speed rotation of materials to allow pressing without the need for pressurizing media. The enhancement of shrinkage by centrifugal force has been empirically demonstrated for liquid-phase sintering of SiO_2. Theoretical prediction of sintering behavior is also attempted based on the modified Kingery model, in which the forces promoting sintering are assumed to be capillary force and centrifugal force. Gradual change in the centrifugal force along the centrifugal direction is taken into account in the modified model. The theoretical model accurately describes the enhancement of shrinkage resulting from centrifugal force, and quantitatively agrees with the experimental results.

Keywords: Centrifugal force; Pressing; Sintering

1. Introduction

Electronic devices are being continuously downsized and thus require ever higher integration patterns. Electroceramics such as layered capacitors, LC filters and actuators are also being miniaturized. Ceramic components provide a great cost advantage in electronic devices and thus incorporate increasing numbers of ceramic parts: for instance, more than 100 capacitors are mounted in cellular phones, of which more than 400 million were sold worldwide in the year 2000.[1] Electroceramics used in common circuits are very small in area, at 1.0×0.5 mm or 0.6×0.3 mm in size.[2] Not only electroceramics but also structural ceramics are increasingly being miniaturized, as seen in the ceramic parts used in micro electric mechanical systems (MEMS).[3,4] In MEMS, a semiconductor etching process is utilized to fabricate complex molds to micrometer-range precision. Casting using molds enables the production of fine ceramic parts such as microrod arrays[3] and turbines.[4] The procedure for the preparation of ceramic MEMS parts is the identical process to that used in most production of ceramics, apart from the scale of the products.

The technological advances mentioned above have led to a need for sintering technology adapted for miniaturized parts. With respect to the enhancement of sintering for such small parts, however, no techniques have yet been developed.

Sintering, which is promoted by pressure, is a diffusion process that minimizes the system surface energy. Hot pressing and hot isostatic pressing are typical sintering processes in which this diffusion is enhanced by applied pressure. These processes can in fact be used to sinter small parts, although sintering molds or capsules are required. Unlike conventional pressing processes, centrifugal motion allows the pressing of materials using their own mass, which has the additional advantage of minimizing any contamination caused by reaction with the mold materials.

Currently, centrifugal force is used in centrifuges that are able to apply acceleration up to 10 Mm/s^2. This acceleration generates a pressure of 400 MPa in a 1-cm cube of Al_2O_3, comparable to that applied in hot isostatic pressing. Centrifugal pressing is similar to uni-axial pressing, except that the pressure changes progressively along the radius of rotation.

* Corresponding author.
E-mail address: y.kinemuchi@aist.go.jp (Y. Kinemuchi).

0955-2219/03/$ - see front matter © 2003 Elsevier Ltd. All rights reserved.
doi:10.1016/S0955-2219(03)00331-5

This particular type of pressure applied by centrifugal force has several visible effects on sintering, such as faster sintering, orientation of crystals, and gradation of microstructures. The present paper focuses on the enhancement of liquid-phase sintering by the use of centrifugal force. A theoretical approach to the enhancement of shrinkage by centrifugal sintering is proposed, which is also validated empirically.

2. Theory of liquid-phase centrifugal sintering

The capillary force originating in the liquid between the particles promotes liquid-phase sintering. Due to the applied force, pressure is exerted on the contact area between the particles, resulting in a chemical potential gradient. As a result, diffusion of atoms takes place along the gradient, leading to morphological changes in the particles. Other pressures, similar to those seen in hot pressing or hot isostatic pressing contribute to the steepening of this chemical potential gradient. In these cases, the contribution of the applied pressure, P, to the sintering kinetics can be expressed by Eq. (1).[5]

$$\frac{\Delta l}{l_o} = \frac{1}{3}\frac{\Delta v}{v_o} = \left[\frac{3k_2\delta D_L C_o V_o}{r_p^3 RT}\left(\frac{2\gamma_{LV}}{k_1 r_p} + P\right)\right]^{\frac{1}{3}} \cdot t^{\frac{1}{3}} \quad (1)$$

$\Delta l/l_o$: fractional linear shrinkage
k_1, k_2 : geometrical constants
D_L : diffusion coefficient in liquid
V_o : molar volume of dissolving material
r_p : initial particle radius
T : absolute temperature
$\Delta v/v_o$: fractional volume shrinkage
δ : thickness of liquid film
C_o : solubility of solid in liquid
γ_{LV} : liquid–vapor surface energy
R : gas constant
t : sintering time

It should be noted that Eq. (1) applies only to the sintering of spherical particles controlled by the diffusion process.

In order to extend Kingery's theory to centrifugal sintering, in which shrinkage is not uniform, since it depends on the position along the radius, shrinkage of the entire specimen is divided into shrinkage per slice.

$$\frac{\Delta l}{l_o} = \frac{\Delta l_1 + \Delta l_2 + \cdots + \Delta l_i + \cdots + \Delta l_{n-1} + \Delta l_n}{l_o} \quad (2)$$

The shrinkage of each slice is a function of its distance from the surface (ξ_i) and is proportional to the thickness of the slice (Δx_i), giving the following relationship. (cf. Fig. 1).

$$\frac{\Delta l}{l_o} = \frac{1}{l_o}\Big[s(\xi_1)\Delta x_1 + s(\xi_2)\Delta x_2 + \cdots + s(\xi_i)\Delta x_i + \cdots + s(\xi_{n-1})\Delta x_{n-1} + s(\xi_n)\Delta x_n\Big] = \frac{1}{l_o}\sum_i^n s(\xi_i)\Delta x_i \quad (3)$$

The function $s(\xi)$ indicates a shrinkage ratio that is identical to Eq. (1). By taking the limit of Δx to zero, Eq. (3) can be expressed by integration:

$$\frac{\Delta l}{l_o} = \frac{1}{l_o}\int_{l_o} s(x)\mathrm{d}x. \quad (4)$$

Consequently, the linear shrinkage for centrifugal sintering can be expressed as follows.

$$\frac{\Delta l}{l_o} = \frac{1}{3}\frac{\Delta v}{v_o} = \left[\left(\frac{3k_2\delta D_L C_o V_o}{r_p^3 RT}\right)^{\frac{1}{3}} l_o^{-1}\int_{l_o}\left(\frac{2\gamma_{LV}}{k_1 r_p} + k_3\rho x r_r \omega^2\right)^{\frac{1}{3}}\mathrm{d}x\right] \cdot t^{\frac{1}{3}} \quad (5)$$

where k_3, r_r, ρ, and ω are, respectively, geometrical factor, radius of rotation, density of specimen, and angular velocity. For a specimen with a simple shape such as a cylindrical pellet, pressure exerted by centrifugal force (P_{CFS}) can be described as linear function of its length: $P_{CFS} = \beta x$. By integrating Eq. (2) with a substitution for this relation, the linear shrinkage under the centrifugal pressure can be simplified as follows.

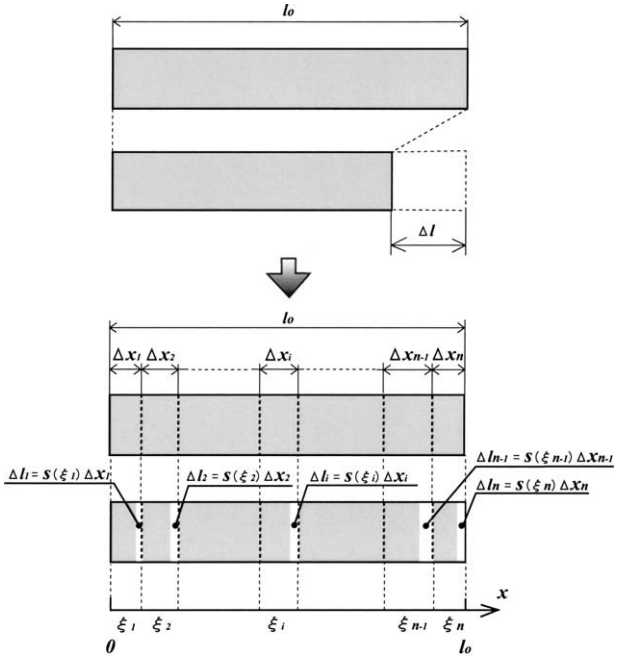

Fig. 1. Shrinkage model for uniform shrinkage (above) and non-uniform shrinkage (below).

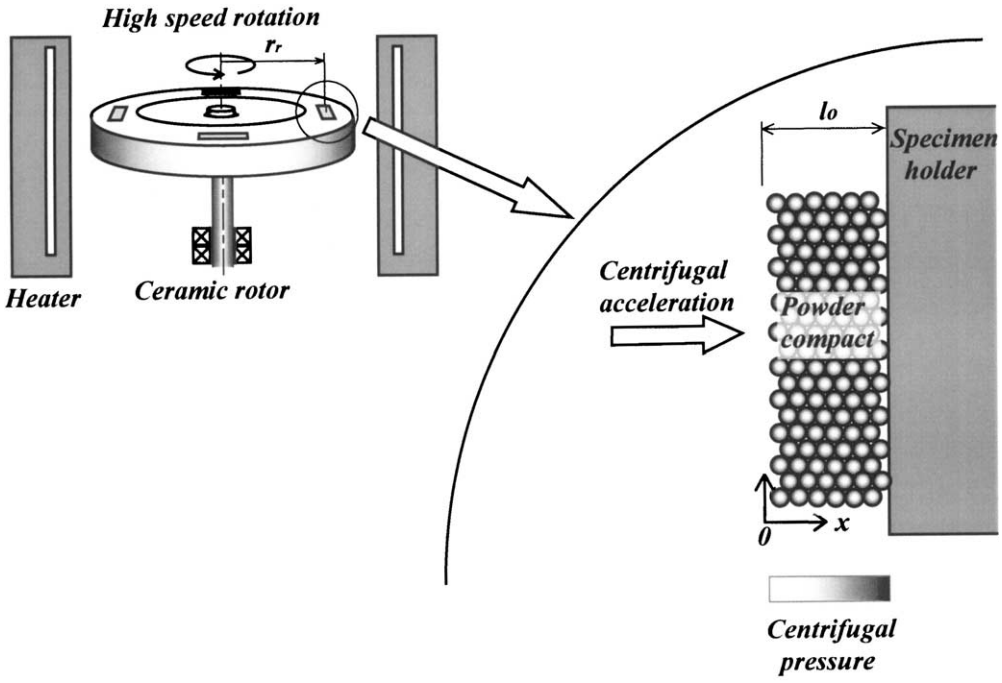

Fig. 2. A model for centrifugal sintering.

$$\frac{\Delta l}{l_o} = \frac{1}{3}\frac{\Delta v}{v_o} = \frac{3}{4}(\gamma t)^{\frac{1}{3}}\frac{P_{CAP}}{\beta l_o}\left[\left(1+\frac{\beta l_o}{P_{CAP}}\right)^{\frac{4}{3}}-1\right] \quad (6)$$

where $\gamma = \dfrac{3k_2\delta D_L C_o V_o P_{CAP}}{r_p^3 RT}$ and $P_{CAP} = \dfrac{2\gamma_{LV}}{k_1 r_p}$.

In short, shrinkage under centrifugal force is proportional to the one-third power of the ratio of the centrifugal to the capillary pressures.

When prismatic particles are sintered, the configuration of particle contact changes, which results in the following relation.

$$\frac{\Delta l}{l_o} = \frac{1}{3}\frac{\Delta v}{v_o} = \frac{5}{6}(\gamma' t)^{\frac{1}{5}}\frac{P_{CAP}}{\beta l_o}\left[\left(1+\frac{\beta l_o}{P_{CAP}}\right)^{\frac{6}{5}}-1\right] \quad (7)$$

As shown in Eqs. (6) and (7), the effect of centrifugal force can be evaluated according to the ratio of pressures. Depending on the geometry of particle contact and the rate-determining process of sintering, the exponent of the pressure ratio is selected, which can be experimentally confirmed by the kinetics of sintering.

3. Experimental

3.1. Equipment

Schematic illustrations of the models of centrifugal sintering and its apparatus used are shown in Figs. 2 and 3, respectively. The centrifugal force is generated by the rotation of a ceramic rotor made of Si_3N_4. The rotor is held by a ball bearing which is airtight by means of magnetic fluid. The motor driving the ceramic rotor rotates at the selected speed, controlled by an inverter circuit. The dimensions of the rotor are 80 mm in radius of rotation and 20 mm in thickness. The specimen is settled in the rotor and subjected to centrifugal force caused by high-speed rotation. The configuration of the specimen setting is shown in Fig. 4. A maximum rotational speed of 10,000 rpm is currently feasible, and will reach 100,000 rpm in the near future. This rotational

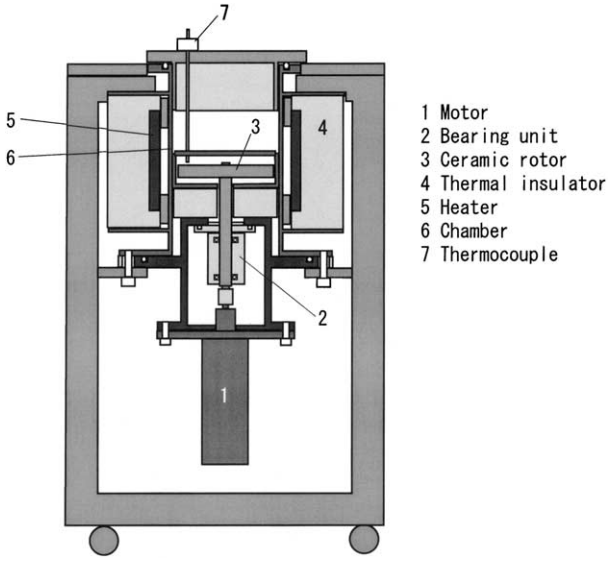

Fig. 3. Experimental apparatus for centrifugal sintering.

unit is installed in a stainless steel chamber, which is heated by a resistance heater. The temperature of the specimen can be raised to 900 °C. The chamber can be evacuated by a rotary pump to a vacuum of 10 Pa. Temperature and rotational speed as a function of time can be controlled and monitored by a computer.

3.2. Material and processing

In the experiments, silica powders with a spherical shape (Fuso Chemical Co., Ltd., SP Series) were used. The diameters of the powders were 0.3 and 4 μm. The powders were dispersed by ultrasonic vibration in distilled water containing dissolved H_3BO_3 and Na_2SiO_2. The composition was chosen to form a liquid phase of 20 mass% at 800 °C according to the phase diagram of the $Na_2B_8O_{13}$–SiO_2 system.[6] The dispersed powders were dried in a rotary evaporator and then sieved through a 90-mesh sieve. Finally, cylindrical pellets with d 11×h 4 mm were prepared by uni-axial pressing under 100 MPa. The density of the pressed pellets was 57% for both powders.

The pellets were placed in the specimen holder with another powder to prevent reaction with the holder and to partly cushion the pressure arising in the tangential direction. Sintering was subsequently carried out at 800 °C in a vacuum of <100 Pa. The heating rate was 5 °C /min and holding time was varied from 1 to 1000 min. Centrifugal force was applied when the temperature reached 800 °C. Acceleration of rotation was 87 km/s^2, which was generated by rotation at 10,000 rpm at a radius of rotation of 80 mm. Sintering without centrifugal force was also carried out as comparison.

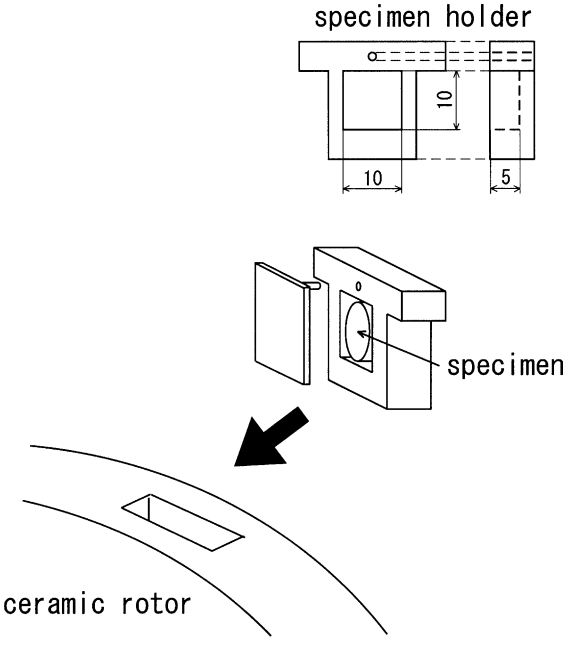

Fig. 4. Specimen setting configuration.

Density was measured by the Archimedean method and used to evaluate sintering kinetics.

4. Results and discussion

As mentioned in Section 2, the kinetics of sintering must be determined to identify the exponent of the pressure ratio in the equations. Fig. 5 shows linear shrinkage as a function of time on a logarithmic scale. Here, initial length was obtained from the density of specimens sintered for 1 min. All the specimens showed a slope of one in five, indicating that diffusion-controlled sintering of prismatic particles had taken place.[7] It is noted that unsuitable definition for the initial length results in different slope in the kinetics, as Prill et al. indicated.[8] Their point is that the unsuitable definition is mainly caused by mixing initial rearrangement process up with middle sintering stage, i.e., the initial length has to be at the moment of middle sintering stage starting. In the present study, liquid phase forms at 730 °C according to the phase diagram. This means that temperature holding at 800 °C had been started after 14 min from the moment of liquid phase formation. During this period, initial rearrangement process is thought to be completed since its kinetics is relatively fast, normally within 10 min for several micron sized powders.[8,9] In addition, the surface tension of liquid phase in the present study is almost constant in the temperature range of 700–800 °C.

As to the kinetics equation for the present case, the enhancement of densification by centrifugal force can be correctly described by Eq. (7). However, the kinetics of sintering is inconsistent with the spherical shape of the particles used as raw powder. The reason was confirmed by direct observation by SEM of the sintered body. The shape of particles after sintering had changed into a prismatic shape as shown in Fig. 6, which explained the

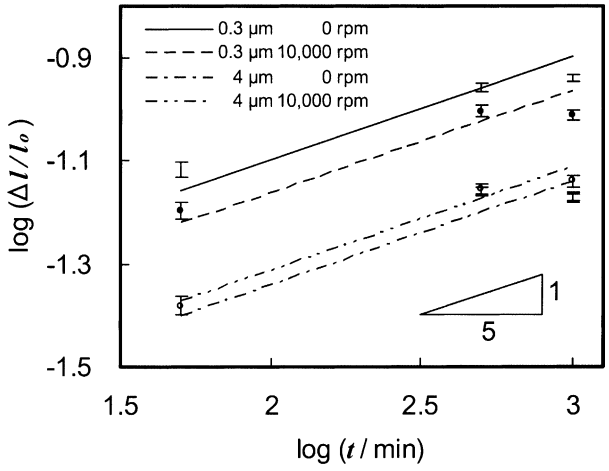

Fig. 5. Linear shrinkage as a function of holding time.

observed kinetics. This change in particle shape arose from crystallization of particles as confirmed by XRD. (See Fig. 7.) The crystal structures before sintering were amorphous, but afterwards showed both quartz and cristobalite phases.

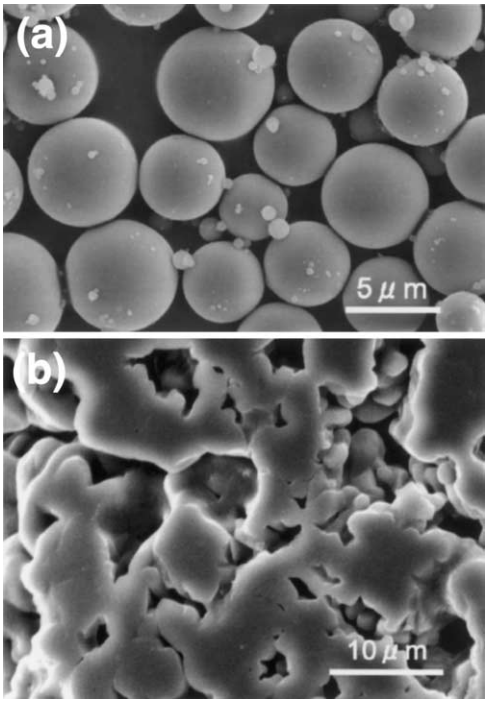

Fig. 6. Morphological change in particle after heating.

Due to the difference in particle size, the capillary force on particles 0.3 μm in size is over ten times greater than that for 4 μm particles, which influences the effect of centrifugal force on the theoretically predicted densification. [See Eq. (6) for the capillary pressure, P_{CAP}] Taking account of the density of specimens with a holding time of 1 min and the amount of liquid phase, the geometrical constant k_1 is estimated to be 0.9. (In addition, k_1 is a factor showing the size ratio between pore radius and particle size.) As a consequence, capillary pressures on particles of 0.3 and 4 μm are calculated to be 3.2 and 0.24 MPa, respectively, assuming a surface energy of 220 mN/m.[10]

As for centrifugal pressure, this is evaluated by the term of βl_o indicating maximum pressure in the specimen. From the acceleration due to rotation, the mass of the specimen and the geometry of the specimen, βl_o is estimated to be 0.46 MPa for all experiments.

The pressure ratio between centrifugal and capillary, $\beta l_o/P_{LPS}$, therefore becomes 0.1 and 1.9 for particle sizes of 0.3 and 4 μm, respectively. Fig. 8 shows the enhancement of densification by centrifugal pressure. Density indicated by the abscissa corresponds to that of without centrifugal pressure, and the ordinate shows density of sintered bodies under centrifugal pressure. Here, sintering time was varied from 1 to 1000 min, which leads different densities due to the progress of sintering. Even though an identical sintering time was adapted for centrifugal sintering and conventional one,

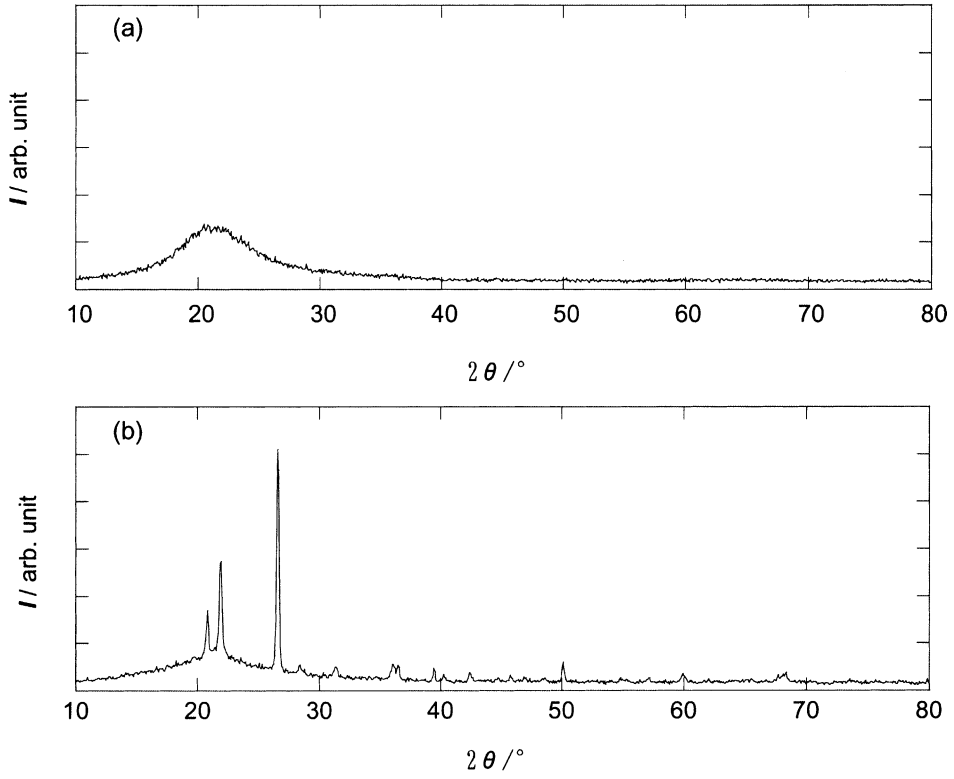

Fig. 7. Crystallization of particle after heating.

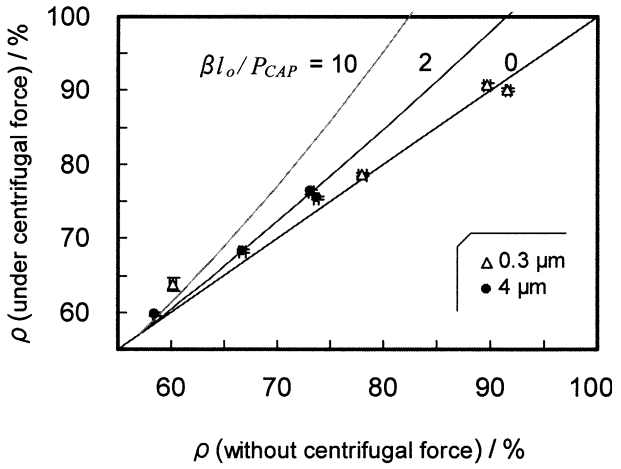

Fig. 8. Enhancement of densification by centrifugal force. Abscissa and ordinate indicate density of specimen sintered without centrifugal force and with centrifugal force, respectively. Lines indicate theoretical prediction based on Eq. (4). The parameter of $\beta l_o/P_{CAP}$ indicates the ratio between centrifugal and capillary pressures that is 0.1 and 1.9 for the powder size of 0.3 and 4 μm, respectively.

resulting density differs each other if the densification is enhanced by centrifugal pressure. For the specimens with a particle size of 0.3 μm, the difference in the densities between both sinterings is not obvious, whereas specimens with 4 μm particle show enhancement of densification by centrifugal sintering with an amount of several %. In this figure, a theoretical prediction using the pressure ratios is also shown. Here, the theoretical calculation was carried out using Eq. (7), where rate constant (γ') being identical to that of conventional sintering was considered. Thus, shrinkage improvement by centrifugal sintering can be evaluated from the difference in shrinkage ratios between both sinterings. A reasonable agreement between the theory and experiment are seen.

In most liquid-phase sintering, capillary pressure reaches several MPa. Hence, a centrifugal force of several tens of MPa or more is effective to enhance densification. When a centrifugal pressure 10 times larger than the capillary pressure is applied, it is possible to obtain a densified body, whereas a density of 80% is acquired without applied centrifugal force, as shown in Fig. 8. Although the centrifugal pressure falls with decreasing specimen size, such pressure is usable in specimens several hundreds of micrometers thick by applying centrifugal acceleration of 10 Mm/s^2. Therefore, the present process can be applied to the fabrication of small ceramic parts such as micro-devices and micro turbines.

5. Summary

Liquid-phase sintering assisted by centrifugal force was examined. Enhancement of shrinkage by the application of centrifugal force was observed. The effect of centrifugal force depends on the ratio between capillary pressure and centrifugal pressure: smaller particles require a higher centrifugal force. This sintering behavior can be qualitatively predicted using a theory based on liquid-phase sintering kinetics that includes the effect of capillary pressure and centrifugal pressure. Owing to the distinctive pressing pattern in centrifugal sintering, the present process is applicable to the sintering of small ceramic parts.

Acknowledgements

The present study was financially supported by the New Energy and Industrial Technology Development Organization (NEDO).

References

1. Nomura, T., Overview and subject of large capacitance multilayer ceramic capacitors. *Bull. Ceram. Soc. Jpn.*, 2001, **36**, 394–398 (in Japanese).
2. Chazono, H., Manufacturing process for Ni-MLCC (Multilayer ceramic capacitor). *Bull. Ceram. Soc. Jpn.*, 2001, **36**, 399–402 (in Japanese).
3. Wang, S., Li, J. F. and Watanabe, R., Fabrication of lead zirconate titanate microrods for 1–3 piezocomposites using hot isostatic pressing with silicon molds. *J. Am. Ceram. Soc.*, 1999, **82**, 213–215.
4. Li, J. F., Sugimoto, S., Tanaka, S., Esashi, M. and Watanabe, R., Manufacturing silicon carbide microrotors by reactive hot isostatic pressing within micromachined silicon molds. *J. Am. Ceram. Soc.*, 2002, **85**, 261–263.
5. Kingery, W. D., Woulbroun, J. M. and Charvat, F. R., Effects of applied pressure on densification during sintering in the presence of a liquid phase. *J. Am. Ceram. Soc.*, 1963, **46**, 391–395.
6. Rockett, T. J. and Foster, W. R., The silica-sodium tetraborate system. *J. Am. Ceram. Soc.*, 1966, **49**, 30–33.
7. Kingery, W. D., Densification during sintering in the presence of a liquid phase. I. Theory. *J. Appl. Phys.*, 1959, **30**, 301–306.
8. Prill, A. L., Hayden, H. W. and Brophy, J. H., A reanalysis of data on the solution-precipitation stage of liquid-phase sintering. *Trans. Met. Soc. AIME*, 1965, **233**, 960–964.
9. Kingery, W. D. and Narasimhan, M. D., Densification during sintering in the presence of a liquid phase. II Experiemental. *J. Appl. Phys.*, 1959, **30**, 307–310.
10. Ahari, K. G., Askari, M. and Cameron, A. M., The surface tension of some sodium borosilicate glasses. *Phys. Chem. Glass*, 1991, **32**, 72–76.